John von Neumann Institute for Computing

Quantum Monte Carlo Simulations of Strong Correlations

Stefan Wessel and Alejandro Muramatsu

published in

NIC Symposium 2006 ,
G. Münster, D. Wolf, M. Kremer (Editors),
John von Neumann Institute for Computing, Jülich,
NIC Series, Vol. **32**, ISBN 3-00-017351-X, pp. 211-218, 2006.

http://www.fz-juelich.de/nic-series/volume32

Quantum Monte Carlo Simulations of Strong Correlations

Stefan Wessel and Alejandro Muramatsu

Institut für Theoretische Physik III
Universität Stuttgart, Pfaffenwaldring 57, 70550 Stuttgart, Germany
E-mail: wessel@theo3.physik.uni-stuttgart.de

We employ large-scale quantum Monte Carlo simulations to study the properties of ultra-cold bosonic atom gases in optical lattices. Based on the stochastic series expansion technique, we analyze the ground state phase diagram of the effective Bose-Hubbard model describing the strongly correlated atom gas. After examining the superfluid to Mott-insulator transition of ultra-cold gases on cubic lattices, we analyze the novel phases induced by extending the setup to include a frustrated lattice geometry or randomness in the interatomic interaction strength. We find that on the triangular lattice the presence of frustration in the underlying lattice leads to the emergence of a supersolid state of matter, due to a novel order-by-disorder effect from a macroscopic degeneracy of the model in the classical limit. Furthermore, we show that the presence of randomness in the interaction strength leads to the formation of a Bose-glass phase of the atoms, and the presence of a tri-critical point in the zero-temperature phase diagram. We discuss possible experimental realization of these scenarios.

1 Strongly Correlated Systems

Strong electronic correlations have become an active research area of solid state physics in the last decades, due to their relevance for e.g. heavy fermion compounds[1], high-temperature superconductors[2], and quantum magnetism[3]. Furthermore, ultra-cold atomic gases in optical lattices provide a new exciting bridge between the physics of these quantum condensed matter systems and the field of quantum optics[4,5]. In the project "Numerical studies of correlated quantum systems" novel numerical schemes are developed and employed to effectively simulate such systems. In addition to the work detailed below, research at the Institut für Theoretische Physik III focuses on the following topics: Efficient quantum Monte Carlo algorithms were constructed, which allow a detailed analysis of the spectral properties of the one-dimensional $t-J$ model[6]. Using large scale numerical simulations, evidence for the presence of spinon, holon and antiholon excitation was provided[6]. Ultra-cold atoms in optical lattices were examined using novel exact numerical methods, which allow for the study of both equilibrium and non-equilibrium properties [7–16]. E.g., a quasi-condensate was found to emerge during free expansion of the atomic cloud out of a Fock state, where the coherent matter wave forms an atom laser[11,15]. Novel numerical techniques were developed and tested at NIC Jülich for the study of time-dependent and non-equilibrium properties of strongly correlated systems, based on the density matrix renormalization group[17]. After successful testing, this method is now applied to a detailed study of coherent matter wave formations of ultra-cold atoms under non-equilibrium conditions. Furthermore, we analyze quantum magnetic systems. In particular, we studied the ground state properties and dynamics of quasiperiodic quantum antiferromagnets[18–20]. Using large scale numerical simulations we also studied thermal and quantum phase transitions in systems of weakly-coupled spin-dimers in the presence of high magnetic fields[22]. We established universal critical properties for the Bose-Einstein condensation (BEC) of

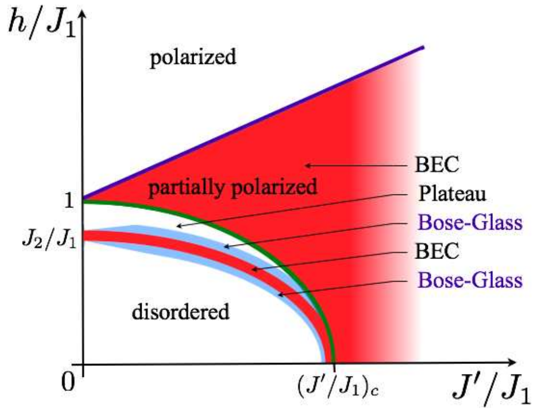

Figure 1. Schematic phase diagram of weakly coupled dimers with a bimodal random distribution of intra-dimer exchange interactions ($J_1 > J_2$) and a weak inter-dimer exchange J' in the presence of an external magnetic field h. Red regions indicate BECs of the magnet excitations, and blue regions the novel Bose-glass phases, emerging from the bond-randomness. $(J'/J_1)_c$ denotes the quantum critical point at $h = 0$ in the absence of randomness.

magnetic excitations in such systems[21], and recently proved the formation of a Bose-glass phase of these magnetic excitations in the presence of randomness[23]. A schematic phase diagram of such a system is shown in Fig 1, exhibiting two Bose-glass phases next to a BEC of magnetic excitations.

2 Ultra-Cold Atom Gases in Optical Lattices

Since the first realizations of BEC in magnetically trapped dilute alkali vapors[24–26], the study of ultra-cold atomic gases (of temperatures down to fractions of microkelvins) has become an active research area of physics. After these first experiments with weakly interacting bosons, among many other achievements the creation of spinor[27] and dipolar[28] condensates has extended the range of observed phenomena. Furthermore, quantum degeneracy was observed in the fermionic case[29], and first steps towards strongly correlated systems have been made[4,5]. Confining the atomic cloud to an optical lattice formed by interfering laser beams leads to physical situations similar to the one encountered in solid state physics[30]. A gas of bosonic atoms under such conditions is described by the Hamiltonian of the Bose-Hubbard model[31],

$$H = -t \sum_{\langle i,j \rangle} \left(b_i^\dagger b_j + h.c. \right) + \frac{U}{2} \sum_i n_i(n_i - 1) + \sum_i V_i n_i. \tag{1}$$

Here, t denotes the nearest neighbor hopping amplitude, and U an on site repulsion between the bosons. Furthermore, b_i ($b_i^\dagger$) denote annilation (creation) operators for bosons on lattice site i, and $n_i = b_i^\dagger b_i$ the local density. The ratio t/U is tuneable by varying the depth of the optical lattice potential[30], which in allows particular to access the regime $U \gg t$ of strongly correlated bosons. V_i denotes a local potential due to the presence of a (usually harmonic) external trapping potential, which confines the atomic gas. In the uniform case ($V_i = 0$), this model has a superfluid phase for low values of U/t and Mott-insulator regions of commensurate densities for stronger interactions[31]. The transition from a superfluid BEC to a Mott-insulator has been achieved for atoms in both one- and three-dimensional optical lattices upon increasing the optical lattice depth[5,32]. Quantum Monte Carlo simulations allow for a qualitative analysis of these experiments.

3 Stochastic Series Expansion Quantum Monte Carlo

We use the stochastic series expansion (SSE) quantum Monte Carlo technique[33,34], which is based on a high temperature series expansion of the partition function Z of the quantum lattice model in Eq. (1) in the inverse temperature $\beta = 1/k_B T$:

$$Z = \mathrm{Tr}\exp(-\beta H) = \sum_{n=0}^{\infty} \frac{\beta^n}{n!} \sum_{\{i_1,\ldots,i_n\}} \sum_{\{b_1,\ldots,b_n\}} \langle i_1| - H_{b_1} |i_2\rangle \cdots \langle i_n| - H_{b_n} |i_1\rangle. \quad (2)$$

The Hamiltonian H is decomposed into a sum of single-bond terms $H = \sum_b H_b$, and we inserted complete sets of basis states. For a bosonic system with a positive hopping amplitude $t > 0$ all terms contributing to Eq. (2) have a positive weight, and thus a Monte Carlo importance sampling of Z can be performed efficiently. Each Monte Carlo step consists of two consecutively applied update schemes: First, in a local, diagonal update, the expansion order n changes by adding/removing diagonal single-bond terms, while keeping the intermediate states and offdiagonal terms fixed. Then in a second, nonlocal update scheme, the offdiagonal terms and intermediate states are modified using a directed loop update scheme[35,36], which allows efficient simulations at low temperatures and quantum phase transitions. The results presented below were obtained using an highly optimized C++ implementation of the algorithm based on the ALPS library[37] with native checkpointing and MPI inter-node communication.

4 The Superfluid to Mott-Insulator Transition

The presence of a magnetic confinement potential in the experiments on bosonic atoms in optical lattices[5,32] leads to spatial confinement and an inhomogeneous density distribution of the atoms inside the trap[30]. The local density of the atoms can however not be measured in current experiments. Instead, absorption images are taken during free expansion of the atomic cloud, which reveal the initial momentum distribution $n(\mathbf{k})$ of the atoms. The gradual loss of interference patterns in such images upon increasing the optical lattice depth gave first indications for the passage from a coherent superfluid BEC to the coexistence of large incoherent Mott-insulator and small superfluid regions[5]. Using quantum Monte Carlo simulations, the corresponding changes in the density distribution of the confined Bose gas inside the optical lattice can be analyzed[38–40]. As an example, in Fig. 2 density distributions are shown for the case of bosons confined to a two-dimensional lattice in (a) the superfluid and (b) the coexistence regime. In the latter case, the strong interactions lead to the formation of a Mott-insulating region with integer density (here $n_i = 1$) at the trap center, surrounded by a superfluid shell. We confirmed the coexistence of superfluid and Mott-insulating regions by analyzing the local compressibility κ in these inhomogeneous

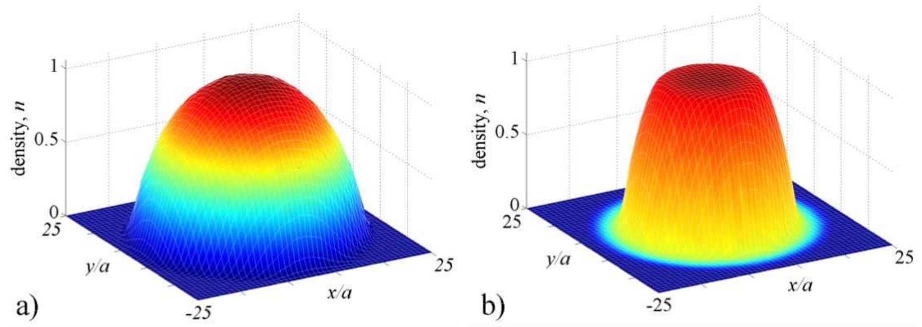

Figure 2. Local density distribution of two-dimensional confined bosonic atoms, (a) in the superfluid phase for $U/t = 6.7$, and (b) in the coexistence regime for $U/t = 25$.

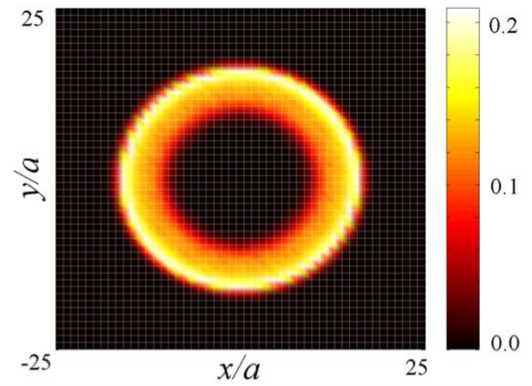

Figure 3. Spatial dependence of the local compressibility κ of bosons confined to a two-dimensional lattice for $U/t = 25$. A superfluid shell surrounds the central Mott-insulator.

systems[38,39]. As an example, the spatial dependence of κ for the case of Fig. 2 b) is shown in Fig. 3, clearly resolving a compressible superfluid ring surrounding the cental incompressible Mott-insulator. In the following, we consider possible extensions of the experimental setup, by including novel lattice geometries and the effects of disorder in our numerical simulations.

5 Supersolid Lattice Bosons

Recently, evidence was reported for a possible supersolid phase of ^{4}He, derived from non-classical momenta of inertia in torsional oscillator experiments[41]. Such a state of matter is characterized by the simultaneous presence of both diagonal and off-diagonal long range order in form of a superfluid with periodic density modulations, breaking both U(1) and

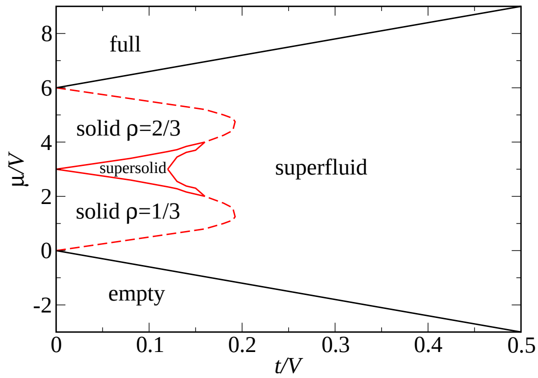

Figure 4. Ground state phase diagram of hard-core bosons on the triangular lattice, obtained from quantum Monte Carlo simulations. Solid lines denote continuous quantum phase transition lines, whereas dashed lines denote first-order transitions. The system is half-filled for $\mu/V = 3$.

translational symmetry[42,43]. Whether the recent observations on ^{4}He are indeed due to the presence of a supersolid state, is still under debate[44–46], and thus the possibility of supersolid phases in translational invariant systems remains unsettled.

Turning to the case of an underlying regular lattice, various proposals have been presented, how to realize a supersolid by loading ultra-cold atoms in optical lattices: such schemes are based on the generation of longer ranged interparticle interactions using dipolar gases[47], Bose-Fermi mixtures[48] or excited states in higher bands[49]. The crystalline order relevant for diagonal long range order in such a supersolid is not the trivial density modulation enforced by the optical lattice but implies an additional superstructure in the bosonic density distribution. Analytical studies using mean-field theory and renormalization group methods indeed found stable supersolid phases in many models, such as the extended Bose-Hubbard model on the square lattice,

$$H = -t \sum_{\langle i,j \rangle} \left(b_i^\dagger b_j + h.c. \right) + V \sum_{\langle i,j \rangle} n_i n_j + \frac{U}{2} \sum_i n_i (n_i - 1) - \mu \sum_i n_i, \qquad (3)$$

in particular in the hard-core limit, $U/V \rightarrow \infty$ close to half-filling. Here, V denotes a nearest-neighbor repulsion and μ the chemical potential of the bosons. However, subsequent numerical calculations showed, that the supersolid state is unstable towards phase separation for $U > 4V$, i.e. for dominant on-site interactions[50,51].

Since it is possible to generate optical lattices which depart from the square lattice geometry[52], the question arises, if stable supersolid phases exist in realistic parameter regimes using different lattice structures. We performed quantum Monte Carlo simulations for the extended Bose-Hubbard model, Eq. (3), on the triangular lattice to study the interplay of supersolidity and geometric frustration[53]. In Fig. 4 we show the phase diagram obtained from our simulations in the hard-core limit.

In addition to the superfluid phase at large values of t/V, the system shows two solid phases for low values of $t/V < 0.2$, with densities $\rho = 1/3$ and $\rho = 2/3$, respectively. We found that upon doping these solid phases towards half-filling, $\rho = 1/2$, two supersolid phases emerge, with a first order transition line at $\rho = 1/2$, separating the low- and high-density supersolids[53]. Supersolidity in this model emerges by an order-by-disorder effect[54] out of a hugely degenerate state of the frustrated classical model at $t = 0$[55], driven by quantum fluctuations[53]. Doping the $\rho = 2/3$ solid with additional bosons (or the $\rho = 1/3$ solid with holes), a possible super-solid is unstable towards phase separation due to the proliferation of domain-walls, giving rise to a first-order transition to the superfluid[53, 51]. Our results are in qualitative agreement with analytical findings[56], which however overestimated the extents of the solid and supersolid phases. While an earlier numerical study[57] did not find a supersolid phase at half-filling, recent studies confirm our calculations[58, 59].

Our preliminary results for the case of hard-core bosons on the Kagomé-lattice, for which a supersolid phase was obtained in spin-wave approximation[56], indicate that the increased quantum fluctuations destroy supersolidity. Compared to the case of the square lattice, the triangular lattice thus offers the experimentally easiest possibility for realizing order-by-disorder phenomena and supersolid phases of ultra-cold atoms on optical lattices.

6 Bosons with Random Interaction Strength

Another means of realizing novel quantum phases of bosons in optical lattices is randomness produced by e.g. additional incommensurable lattices[60], or by laser speckles[61]. They can lead to Anderson localization[62] and Bose-glass phases[31].

We proposed a novel means of realizing randomness for bosons in optical lattices, by employing the extreme sensitivity of the bosonic scattering potential at the verge of a Feshbach resonance[63, 64], leading to a random interaction strength U in the Bose-Hubbard model[65]. In our scenario bosons on an atom chip[66] are considered close to an electric wire, producing a spatially random magnetic field[66]. This will induce random variations in the local interaction strength, if the bosons are set near the Feshbach resonance by the overall off-set field[65]. We studied the phase diagram of the one-dimensional random-U Bose-Hubbard model using both a strong coupling expansion (SCE)[67] and SSE quantum Monte Carlo simulations[65], and contrasted our model to the case of randomness in the chemical potential[31]. The resulting zero-temperature phase diagram for a uniformly distributed interaction strength, $U(1-\epsilon) \leq U_i \leq U(1+\epsilon)$, is shown in Fig. 5 for $\epsilon = 0.25$. Similar to the case of a random chemical potential[31], the disordered system exhibits a Bose-glass regime, identified as an insulating, but compressible phase. However, in the random-U case, the disorder selectively destroys all Mott-insulating regions above an ϵ-dependent filling factor ($n \geq 3$ for $\epsilon = 0.25$). Furthermore, we find that the Bose-glass phase does not extend into the low-density region of the phase diagram, $\mu < 0$, giving rise to a tricritical point along the lower boundary of the $n = 1$ Mott-lobe. Estimates of the relevant length scales indicate that our scenario can indeed be realized using currently available experimental techniques[65].

Acknowledgments

We wish to thank HLRS-Stuttgart (Project CorrSys) and NIC Jülich for the allocation of computer time.

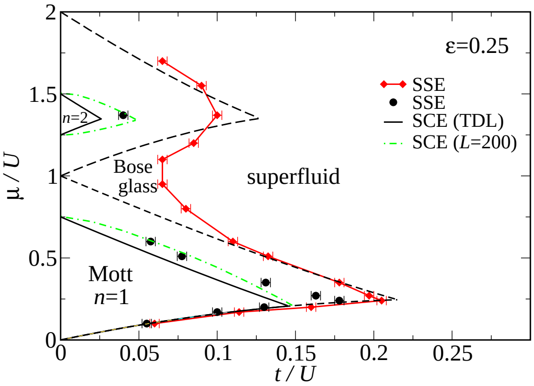

Figure 5. Zero-temperature phase diagram of bosons on a one-dimensional optical lattice with random interaction strength of $\epsilon = 0.25$, obtained from SSE simulations of 200 sites and a third-order SCE for the thermodynamic limit (TDL). The extent of the Mott-lobes in the pure case ($\epsilon = 0$) from SCE is indicated by the dashed line, whereas the dot-dashed line shows the SCE results for a finite system of $L = 200$ sites.

References

1. P. Fulde, J. Keller and G. Zwicknagl, Solid State Physics - Advances in Research and Applications **41**, 1 (1988).
2. J. G. Bednorz and K. A. Müller, Z. Phys. B **64**, 189 (1986).
3. U. Schollwöck, J. Richter, D. J. J. Farnell and R. F. Bishop (Eds.), *Quantum Magnetism*, Lecture Notes in Physics 645, Springer, Berlin (2004).
4. B. Paredes *et al.*, Nature **429**, 277 (2004).
5. M. Greiner *et al.*, Nature **415**, 39 (2002).
6. C. Lavalle *et al.*, Phys. Rev. Lett. **90**, 216401 (2003).
7. M. Rigol *et al.*, Phys. Rev. Lett. **91**, 130403 (2003).
8. M. Rigol, A. Muramatsu, Phys. Rev. A **69**, 053612 (2004).
9. M. Rigol and A. Muramatsu, Phys. Rev. A **70**, 031603(R) (2004).
10. M. Rigol and A. Muramatsu, Phys. Rev. A **70**, 043627 (2004).
11. M. Rigol and A. Muramatsu, Phys. Rev. Lett. **93**, 230404 (2004).
12. M. Rigol and A. Muramatsu, Opt. Commun. **243**, 33 (2004).
13. M. Rigol and A. Muramatsu, Phys. Rev. Lett. **94**, 240403 (2005).
14. M. Rigol and A. Muramatsu, Phys. Rev. A **72**, 013604 (2005).
15. M. Rigol and A. Muramatsu, Mod. Phys. Lett. B bf 19, 861 (2005).
16. M. Rigol *et al.*, Phys. Rev. Lett. **95**, 218901 (2005).
17. S. R. Manmana, A. Muramatsu, and R. M. Noack, AIP Conf. Proc. **789**, 269 (2005).
18. S. Wessel, A. Jagannathan, and S. Haas, Phys. Rev. Lett. **90**, 177205 (2003).
19. S. Wessel, and I. Milat, Phys. Rev. B **71**, 104427 (2005).
20. S. Wessel, Phys. Rev. Lett. **94**, 029701 (2005).
21. O. Nohadani *et al.*, Phys. Rev. B **69**, 220402(R) (2004).
22. O. Nohadani, S. Wessel, and S. Haas, Phys. Rev. B **72**, 024440 (2005).
23. O. Nohadani, S. Wessel, and S. Haas, Phys. Rev. Lett. **95**, 227201 (2005).
24. M. H. Anderson *et al.*, Science **269**, 198 (1995).

25. C. C. Bardley *et al.*, Phys. Rev. Lett. **75**, 1687 (1995).
26. K. B. Davis *et al.*, Phys. Rev. Lett. **75**, 3969 (1995).
27. J. Stenger *et al.*, Nature **396**, 345 (1999).
28. A. Griesmaier *et al.*, Phys. Rev. Lett. **94**, 160401 (2005).
29. B. DeMarco and D. S. Jin, Science **285**, 1703 (1999).
30. J. Jaksch *et al.*, Phys. Rev. Lett. **81**, 3108 (1998).
31. M. P. A. Fisher *et al.*, Phys. Rev. B **40**, 546 (1989).
32. T. Stöferle *et al.*, Phys. Rev. Lett. **91** 130403 (2004).
33. A. W. Sandvik and J. Kurkijärvi, Phys. Rev. B **43**, 5950 (1991).
34. A. W. Sandvik, Phys. Rev. B **59**, R14157 (1999).
35. O. F. Syljuåsen and A. W. Sandvik, Phys. Rev. E **66**, 046701 (2002).
36. F. Alet, S. Wessel, and M. Troyer, Phys. Rev. E **71**, 036706 (2005).
37. F. Alet *et al.*, J. Phys. Soc. Jpn. Suppl. **74**, 30 (2005); source codes available at `http://alps.comp-phys.org/`.
38. S. Wessel, *et al.*, Adv. Solid State Phys. **44**, 265 (2004).
39. S. Wessel, *et al.*, Phys. Rev. A **70**, 053615 (2004).
40. S. Wessel, *et al.*, J. Phys. Soc. Jpn. Suppl. **74**, 10 (2005).
41. E. Kim and M. H. W. Chan, Nature **427**, 225 (2004); Science **305**, 1941 (2004).
42. O. Penrose and L. Onsager, Phys. Rev. **104**, 576 (1956).
43. A. J. Leggett, Phys. Rev. Lett. **25**, 1543 (1970).
44. A. Leggett, Science **305**, 1921 (2004).
45. N. Prokof'ev and B. Svistunov, Phys. Rev. Lett. **94**, 155302 (2005).
46. E. Burovski *et al.*, Phys. Rev. Lett. **94**, 165301 (2005).
47. K. Góral, L. Santos and M. Lewenstein, Phys. Rev. Lett. **88**, 170406 (2002).
48. H. P. Büchler and G. Blatter, Phys. Rev. Lett. **91**, 130404 (2003).
49. V. W. Scarola and S. Das Sarma, Phys. Rev. Lett. **95**, 03303 (2005).
50. G. G. Batrouni and R. T. Scalettar, Phys. Rev. Lett. **84**, 1599 (2000).
51. P. Sengupta *et al.*, Phys. Rev. Lett. **94**, 207202 (2005).
52. L. Santos *et al.*, Phys. Rev. Lett. **93** 030601 (2004).
53. S. Wessel and M. Troyer, Phys. Rev. Lett. **95**, 127205 (2005).
54. J. Villain *et al.*, J. Phys. **41**, 1263 (1980).
55. G. H. Wannier, Phys. Rev. **79**, 357 (1950).
56. G. Murthy, D. Arovas and A. Auerbach, Phys. Rev. B **55**, 3104 (1997).
57. M. Boninsegni, J. Low Temp. Phys. **132**, 39 (2003).
58. D. Heidarian and K. Damle, Phys. Rev. Lett. **95**, 127206 (2005).
59. R. Melko *et al.*, Phys. Rev. Lett. **95**, 127207 (2005).
60. R. B. Dimer *et al.*, Phys. Rev. A **64**, 033416 (2001).
61. P. Horak, J.-Y. Courtois and G. Grynberg, Phys. Rev. A **58**, 3953 (2000).
62. P. W. Anderson, Phys. Rev. B **109**, 5 (1958).
63. E. Tiesinga *et al.*, Phys. Rev. A **47**, 4114 (1993).
64. S. Inouye *et al.*, Nature **392**, 151 (1998).
65. H. Gimperlein, S. Wessel, J. Schmiedmayer, and L. Santos, Phys. Rev. Lett. **95**, 170401 (2005).
66. S. Wildermuth *et al.*, Nature **435**, 440 (2005).
67. J. K. Freericks and H. Monien, Phys. Rev. B **53**, 2691 (1996).